Proceedings of ASME Turbo Expo 2011
GT2011
June 6-10, 2011, Vancouver, British Columbia, Canada

GT2011-45167

RESEARCH OF A NEW DESIGN METHOD OF VARIABLE AREA NOZZLE TURBINE FOR VCE — HARMONIC DESIGN METHOD

FANG Xiang-jun[1], YIN Zhao[1], LIU Si-yong[1], WANG Ping[1], LIU Zhi-gang[2]
1 Beihang University, Beijing 100191, P. R. China
2 Civil Aviation University of China, Tianjin 300300, P. R. China
E-mail: turbinebuaa@buaa.edu.cn

ABSTRACT

A new design method of variable area nozzle turbine (VANT) for Variable Cycle Engine (VCE) was expounded and researched in the paper. It is named as Harmonic Design Method, the purpose of which is to reach the demands of a series of objective conditions for the VCE turbine. Two turbines were designed using the present method and an original method discussed before. The characteristic maps of the two turbines were acquired by 3D numerical simulations to verify the feasibility and superiority of harmonic design method. Then specific analysis of the flows in two turbines under different objective conditions is performed. The results show that the turbine has good aerodynamic performance for all kinds of working conditions and reaches the design demands as well, and the flow fields are more reasonable in the turbine by harmonic design method than the original one.

INTRODUCITON

VCE is the unique aero-engine which can change its thermodynamic cycle parameters by means of adopting variable geometry components [1]. It enables the aircraft to cruise on both supersonic and subsonic conditions with utmost Specific Fuel Consumption (SFC).There are many measures to adjust the massflow rate and expansion ratio of turbine in order to adapt it to different operating conditions of VCE. In this paper, both massflow and expansion ratio are adjusted by controlling the guide vane throat area, which depends on the vane stagger angle.

An experiment of the application of VANT on turbo jet engine was performed early in 1953 [2], the results of which showed that the efficiency decreased with lower and greater stagger angles compared to the design condition and it was evident that considerable change in such flow conditions as choking point, efficiency, reaction, surface velocity, etc., occurred as variable geometry was imposed on a turbine. NASA equipped VCE engine YJ101 with variable area nozzle turbine in low pressure stage [3], and the performance was successful from both a mechanical and aerodynamic point of view and the excellent stall margin of the compression elements allowed a wide stall-free range of flow matching. HYPR project hold by Japan was launched in 1989 and the combined cycle engine (CCE), comprised of variable cycle turbo jet engine and ramjet, was able to acquire 15% more thrust by changing the stagger angle of the low pressure turbine nozzle. The fourth generation VCE in progress will adopt new technique in high pressure stage to control the nozzle area other than the conventional VANT to decrease the tip leakage loss, and the SFC is predicted to be 10%-15% lower than the conventional turbo jet in partial power condition [4].

It can be seen that the VANT plays a more and more important role in modern airplane engine. But there is great difference between the VCE turbine and conventional one whose guide vanes are rotated. It is more complex and difficult for the VCE turbine because it runs in wider working envelops by far than conventional turbine and must meet all demands under a series of different long-term working conditions. Therefore, the conventional turbine is usually given only one objective condition which is treated as design condition whereas the VCE turbine must be given a series of objective conditions. At the same time, VANT has a variable geometry, so it’s more complicate to design than other parts of VCE such as the high pressure turbine [5].

A new design method, named as *Harmonic Design Method*, was introduced to reach the aims of a series of objective conditions for the VCE turbine. According to the method, the characters of all design conditions must firstly be analyzed, then a set of parameters similar with all objective conditions are calculated as the design condition, therefore most objective conditions are considered in the harmonic method.

To verify the theory, a testing VCE turbine was designed by the method. Six characteristic maps of turbine are simulated by CFD tools when the vane is located at six different positions by changing the vane stagger angle. The new turbine is also compared with the original one, which verifies that the flow fields are more reasonable in the turbine by harmonic method.

DESIGN METHOD

One of advantages of VCE is that it can work on a series of flight conditions so as to keep low SFC and high efficiency when it adjusts its bypass ratio and thermodynamics cycle parameters by operating system. But at the same time, the compressor also changes its conditions, and the turbine must adapt to the alterations which means that the turbine must keep high efficiency even if it works in greatly different conditions, which we call as the objective conditions in order to match the compressor. Thus the turbine corresponds with *m* series of parameters as follows:

Condition *1*	$P^*_{in,1}$	$T^*_{in,1}$	G_1	μ_1	n_1	$\pi^*_{T,1}$	$\geq \eta^*_{T,1}$
Condition *2*	$P^*_{in,2}$	$T^*_{in,2}$	G_2	μ_2	n_2	$\pi^*_{T,2}$	$\geq \eta^*_{T,2}$
……	……						
Condition *i*	$P^*_{in,i}$	$T^*_{in,i}$	G_i	μ_i	n_i	$\pi^*_{T,i}$	$\geq \eta^*_{T,i}$
……	……						
Condition *m*	$P^*_{in,m}$	$T^*_{in,m}$	G_m	μ_m	n_m	$\pi^*_{T,m}$	$\geq \eta^*_{T,m}$

For conventional turbine, its geometry doesn't change. The stagnant efficiency of design condition is depended on equation 1:

$$\eta^*_T = f_1(G\sqrt{T^*_{in}}/P^*_{in}, n/\sqrt{T^*_{in}}) = f_1(\bar{G}, \bar{n}) \quad (1)$$

For VCE turbine, there are a series of reduced mass flow and reduced wheel speed:

Condition *1*	$f_1(G_1\sqrt{T^*_{in,1}}/P^*_{in,1}, n_1/\sqrt{T^*_{in,1}})$
Condition *2*	$f_2(G_2\sqrt{T^*_{in,2}}/P^*_{in,2}, n_2/\sqrt{T^*_{in,2}})$
……	……
Condition *i*	$f_i(G_i\sqrt{T^*_{in,i}}/P^*_{in,i}, n_i/\sqrt{T^*_{in,i}})$
……	……
Condition *m*	$f_m(G_m\sqrt{T^*_{in,m}}/P^*_{in,m}, n_m/\sqrt{T^*_{in,m}})$

We can rotate the nozzle to adjust the throat area to meet all conditions including reduced mass flow and reduced wheel speed.

A condition among all the objective conditions is chosen as the design condition according to the original design method. Then the turbine is designed according to the set of design parameters. The other objective conditions can be gotten by rotating the stagger angle of nozzle.

Namely:

$$\bar{G}_d \in (\bar{G}_1, \bar{G}_2, \cdots, \bar{G}_i, \cdots, \bar{G}_m) \quad (2)$$

$$\bar{n}_d \in (\bar{n}_1, \bar{n}_2, \cdots, \bar{n}_i, \cdots, \bar{n}_m) \quad (3)$$

$$\pi^*_{T,d} \in (\pi^*_{T,1}, \pi^*_{T,2}, \cdots, \pi^*_{T,i}, \cdots, \pi^*_{T,m},) \quad (4)$$

The original method can solve the problem of multi-aim conditions but the attack angle of gas may cause high dynamic loss because of the rotated nozzle. However, in the new design method, all objective conditions are weighted and a new design condition can be acquired as follows.

$$\pi^*_{T,d} = (P^*_{in}/P^*_{out})_d = \sum_{i=1}^{m} w_i \pi^*_{T,i} \quad (5)$$

$$\bar{G}_d = (G\sqrt{T^*_{in}}/P^*_{in})_d = \sum_{i=1}^{m} w_i \bar{G}_i \quad (6)$$

$$\bar{n}_d = (n/\sqrt{T^*_{in}})_d = \sum_{i=1}^{m} w_i \bar{n}_i \quad (7)$$

$$\bar{L}_d = (L/P^*_{in}\sqrt{T^*_{in}})_d = \sum_{i=1}^{m} w_i \bar{L}_i \quad (8)$$

w_i (i=1,2,⋯,m) are the weighted factors and the sum of them is 1. The weighted factors can be set by the importance of objective conditions.

Therefore,

$$\bar{G}_d \notin (\bar{G}_1, \bar{G}_2, \cdots, \bar{G}_i, \cdots, \bar{G}_m) \quad (9)$$

$$\bar{n}_d \notin (\bar{n}_1, \bar{n}_2, \cdots, \bar{n}_i, \cdots, \bar{n}_m) \quad (10)$$

$$\pi^*_{T,d} \notin (\pi^*_{T,1}, \pi^*_{T,2}, \cdots, \pi^*_{T,i}, \cdots, \pi^*_{T,m},) \quad (11)$$

However, this set of new parameters has taken into account the influences of all the objective conditions. We call it as Harmonic Design Method.

In fact, the stagger angle of nozzle is very important for the performance of turbine. Therefore, the characteristic maps of turbine include the affection of the stagger angle.

$$\eta^*_T = f_2(G\sqrt{T^*_{in}}/P^*_{in}, n/\sqrt{T^*_{in}}, \Delta\lambda) = f_2(\bar{G}, \bar{n}, \Delta\lambda) \quad (12)$$

In this paper, a suite of new data was acquired by weighting the dimensionless parameters under low bypass ratio mode and high bypass ratio mode. The new condition is then used as the design condition. A three-dimensional (3D) profile design method based on S_1 stream surface [6] was applied, and the profile of the stator and rotor are shown below.

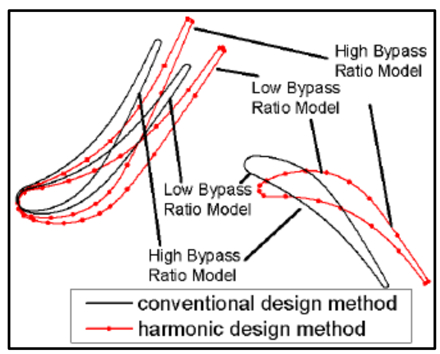

Figure 1. Profiles at mid-span of both turbines using two design methods

It's can be seen that, the new turbine has a positive attack angle in the high bypass ratio mode and a negative one in the low bypass ratio mode, which prevent severe separation on the suction side for both stator and rotor, while the attack angle in both modes are positive in the old turbine. The new turbine also has longer axial chord to reduce large turning angle.

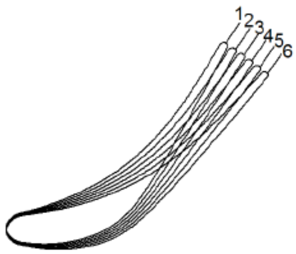

Figure 2. Six positions of stator under different stagger angles

Six positions of the stator are shown in Fig. 2. Position 1 and 6 corresponds to the high bypass ratio mode and low bypass ratio mode respectively, while other positions are acquired by averaging the variation range of the stagger angle into 5 parts.

ANALYSIS OF TURBINE CHARACTIRISTIC

NUMECA/FINE is used to generate the grids and to calculate the flows in the turbines. The flow field of each blade was divided into 5 blocks. The mesh around the blade was O-type and y+ in the innermost layer was verified less than 10, and other blocks were H-type. The flows of turbine under different operating conditions were simulated by solving the steady Reynolds averaged N-S equation using S-A one equation model. Central difference scheme is applied in space, and local time step and multi-grid technique are used to accelerate convergence. Total pressure and total temperature at inlet and static pressure at outlet are given as boundary conditions.

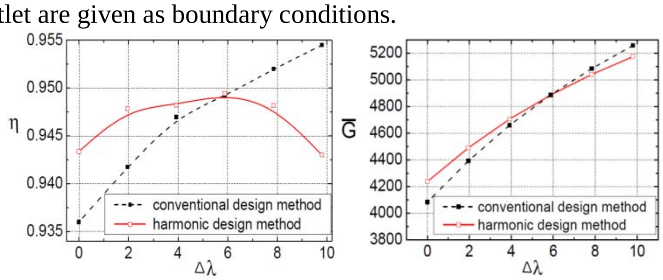

(a) Efficiency (b) Massflow

Figure 3. Performance of turbine under different stagger angles at design speed and expansion ratio

Different efficiencies under different stagger angles at design speed and expansion ratio using conventional design method and harmonic design method are show respectively in Fig. 3-a.

The efficiency line of original turbine increases monotonically with stagger angle, while acquires the maximum in low bypass ratio mode. However, the efficiency of the turbine using harmonic design method reaches the maximum in the middle section of the whole variation region and the values in low bypass ratio mode and high bypass ratio mode are almost same. It's clear that the efficiency of the original turbine decreases sharply as the stagger angle decreases, indicating that the original turbine is susceptible to the stagger angle. But the performance of the new turbine doesn't vary much under different stagger angles, which is more appropriate for VANT of VCE to meet the demand of high efficiency under different conditions. Numerically, the efficiencies in low bypass ratio mode and high bypass ratio mode are 95.45% and 93.64% in the original turbine, 94.34% and 94.17% in the new one.

It increases linearly with the increase of the stagger angle for both turbines, so it's effective to change the stagger angle to control the flow capacity. The flow curve of new turbine with small slope is also able to satisfy the flow demand and balance the two objective conditions better. In order to analyze the new turbine more deeply, efficiency characteristics under different stagger angles is shown below.

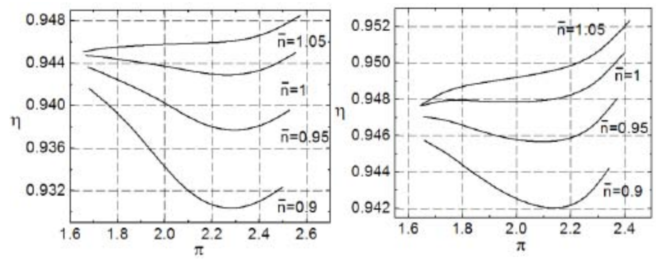

(a) $\triangle\lambda=0$ $\pi_d=2.089$ (b) $\triangle\lambda=1.96$ $\pi_d=1.995$

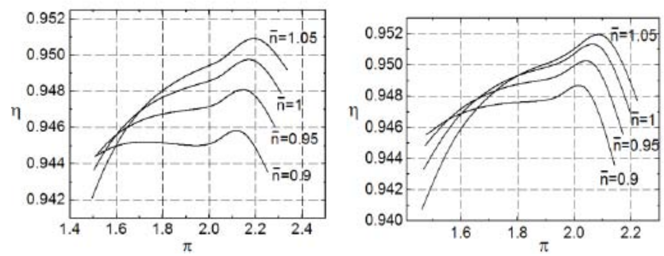

(c) $\triangle\lambda=3.92$ $\pi_d=1.905$ (d) $\triangle\lambda=5.88$ $\pi_d=1.818$

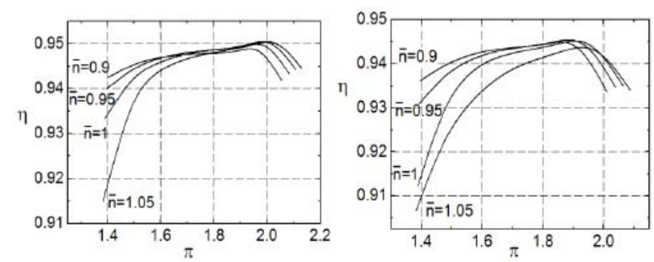

(e) $\triangle\lambda=7.84$ $\pi_d=1.734$ (f) $\triangle\lambda=9.8$ $\pi_d=1.653$

Figure 4. Efficiency characteristics under different stagger angles

The relative speeds are respectively 0.9, 0.95, 1 and 1.05. There are great differences in the efficiency characteristics with different stagger angles as shown in Fig. 4. The efficiency decreases first and arises later with expansion ratio under lower stagger angle such as in Fig. 4-a and Fig. 4-b. Meanwhile, it increases with the relative speed at the same expansion ratio. On the contrary, the efficiency decreases after an initial increase with expansion ratio when the stagger angle is bigger. The performance of turbine at low expansion ratio gets worse as the stagger angle increases and the difference in efficiency is much greater at larger stagger angles as the speed is varied. It can be inferred that the most satisfactory result should be in the turbine with the stagger angle in the middle section of the variation, which is achieved by the harmonic method.

Although the efficiency of turbine between high bypass ratio mode and low bypass ratio mode doesn't vary much under the design speed and design expansion ratio, the performances under other conditions differ a lot such as the variation behavior of the ratio, the variation behavior of the speed and the fluctuation range. More attention should be paid on the turbine in low bypass ratio mode with negative attack angle.

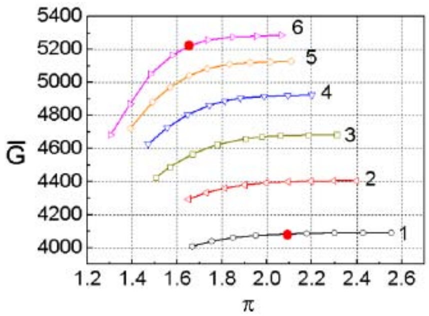

Figure 5. Flow rate characteristics under different stagger angles

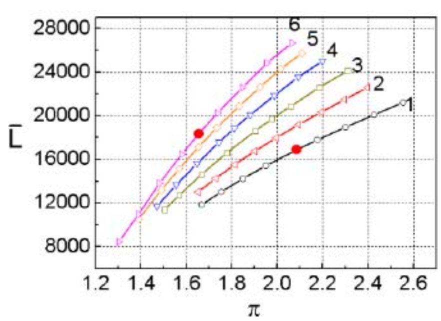

Figure 6. Power characteristics under different stagger angles

For each stagger angle, the mass flow tends to the chocking point as the expansion increases, and the turbines under two objective conditions are unchoked as shown in Fig. 5. The flow capacity rises as the stagger angle increases at the same expansion ratio while the increasing speed gets slow. As the stagger angle gets bigger, the expansion ratio corresponding to choking point becomes lower because the expanding effect is also reduced as the throat gets larger.

The reduced power increases almost linearly with the increase of expansion ratio under each stagger angle as shown in Fig. 6. The turbine with larger stagger angle has a better work capacity.

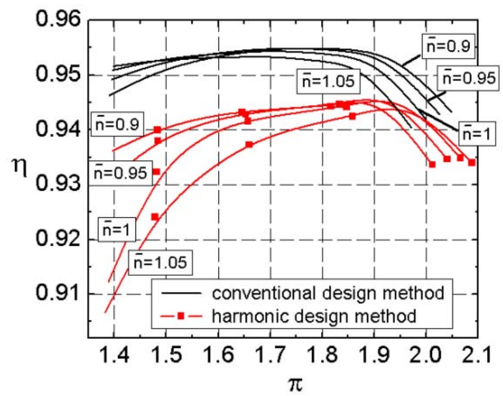

(a) Low bypass ratio mode

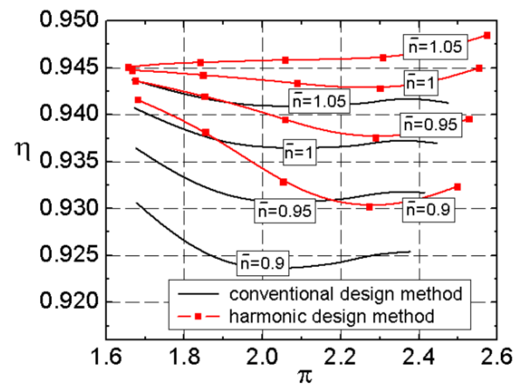

(b) High bypass ratio mode

Figure 7. Efficiency characteristic maps in two modes of two turbines

The efficiency characteristic maps shown in Fig. 7 represent the performance difference in two turbines using different design methods. In general, the original turbine behaves better in the low bypass ratio mode and worse in the high bypass ratio mode. In the low bypass ratio mode, the original turbine has good performance in the design condition, and the efficiency maintains high with the variation of the expansion ratio and relative speed. However, the efficiency of the new turbine has a wide range of fluctuation especially with high relative speed and drops quickly as the expansion ratio decreases, from which it can be seen that the new turbine is sensitive to the variation of the attack angle in low bypass ratio mode. In high bypass ratio mode, both of turbines are stable as the expansion ratio changes. The flows under design condition in both modes for both turbines are analyzed as follows.

ANALYSIS OF FLOWS IN HIGH AND LOW BYPASS RATIO MODES

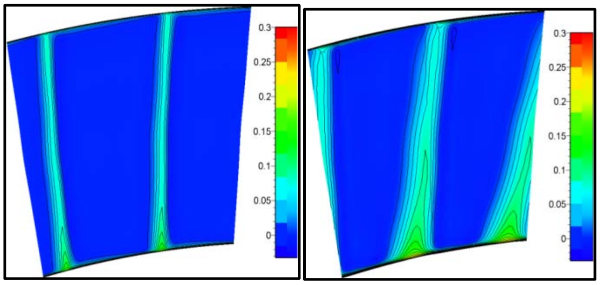

(a) Low bypass ratio mode (b) High bypass ratio mode

Figure 8. Total pressure loss contours at stator outlet for conventional design method

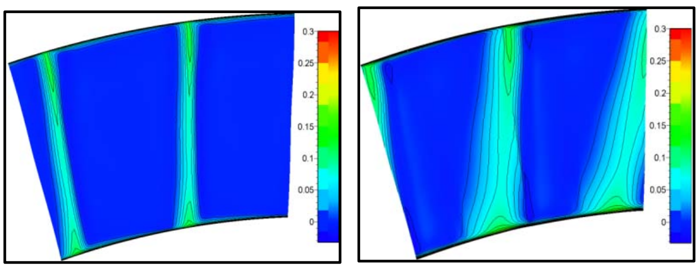

a) Low bypass ratio mode (b) High bypass ratio mode

Figure 9. Total pressure loss contours at stator outlet for harmonic design method

Total pressure loss is defined as:

$$\xi = (P_{in}^{*} - P^{*})/P_{in}^{*} \tag{13}$$

Both turbines have wider wake region in high bypass ratio mode compared to low bypass ratio mode, and ξ in high and low bypass ratio mode are 0.79% and 1.87% in original turbine, 0.988% and 2.26% in new turbine. It can be seen that the loss in the tip is larger for the new turbine, meanwhile the low energy flows in the hub of the original stator is more obvious.

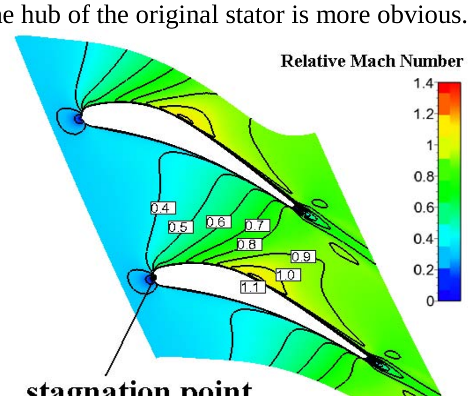

(a) Low bypass ratio mode

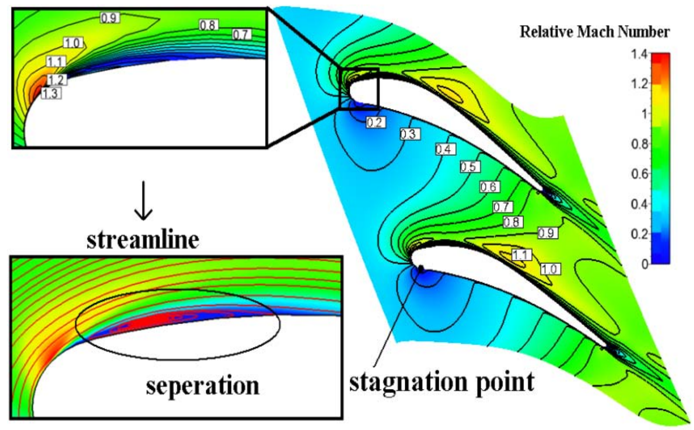

(b) High bypass ratio mode

Figure 10. Distribution of relative Mach number and streamline at 50% span of the original turbine

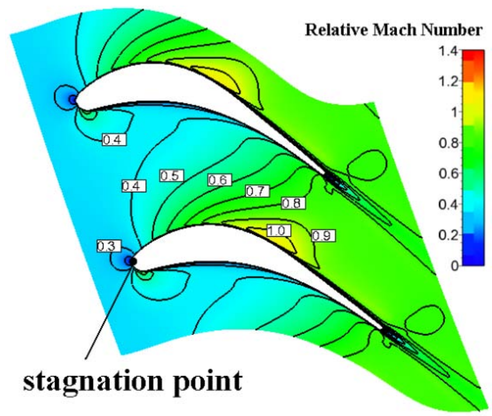

(a) Low bypass ratio mode

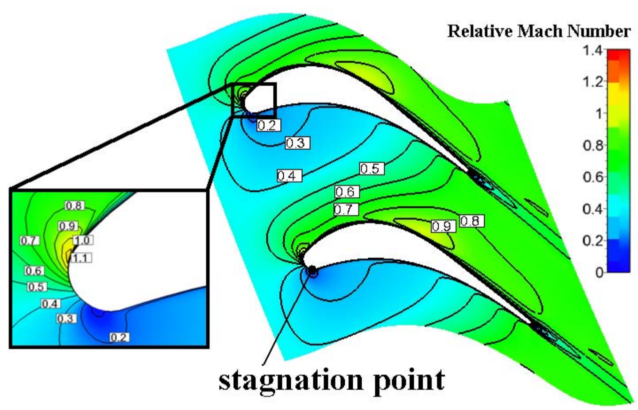

(b) High bypass ratio mode

Figure 11. Distribution of relative Mach number and streamline at 50% span of the new turbine

The attack angle of the rotor of original turbine is almost zero in the low bypass ratio mode which is also the design condition as shown in Fig. 10-a. But when it comes to the high bypass ratio, the attack angle is so large that severe expansion occurs on the suction side. The shock wave is produced to cause a sudden increase of pressure, and the boundary becomes thick. Then the shock wave boundary interaction leads to the separation after shock wave. The maximum Mach number even exceeds 1.4. Meanwhile, the new turbine rotor has a stronger ability to adapt the variation of the attack angle caused by the rotation of the stator. Separation is not found in low bypass ratio mode although the pressure of the air on the pressure side region is low as a result of negative attack angle. In high bypass ratio mode, the expansion effect is not as strong as the original turbine and the air sticks to the blade well. The maximum Mach number in the shock wave region is 1.2.

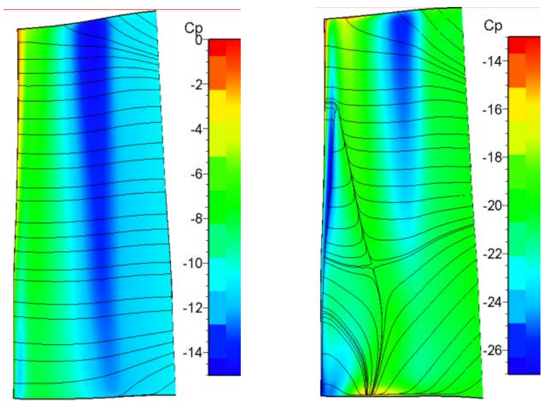

(a) Low bypass ratio mode (b) High bypass ratio mode

Figure 12. Distribution of limiting streamline and pressure coefficient on suction side of the original turbine rotor

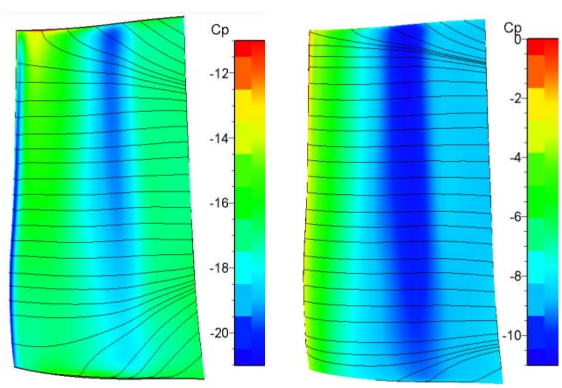

(a) Low bypass ratio mode (b) High bypass ratio mode

Figure 13. Distribution of limiting streamline and pressure coefficient on suction side of the new turbine rotor

The pressure coefficient is defined as follows:

$$\mathrm{Cp} = (\mathrm{P} - \mathrm{P}_{\mathrm{in}}^{*})/(\,\rho_{\mathrm{in}}\,\mathrm{u}_{\mathrm{in}}^{2}/2) \quad (14)$$

In order to compare the radial secondary flow in both turbine rotors, limiting streamlines are presented in Fig. 12 and Fig. 13. The flow from hub to 75% span in the high bypass ratio mode of the original turbine is deformed. Two radial lines correspond to the beginning line and finishing line of separation caused by big attack angle which was discussed right now. Vortexes with 3D features are generated on both S2 and S1 surfaces to cause thick boundary and the flow is obstructed. The loss is mainly produced by the shock wave, separation and the low energy flow in the hub. Meanwhile, the new turbine performs well in both modes, and the limiting line distributions are more even.

CONCLUSIONS

Harmonic design method, a new design method of VANT for VCE, is introduced in this article and two turbines are acquired respectively using this method and an original method. The efficiency and reduced mass flow plotted as a function of variation of stagger angle for both turbines show that the new turbine behaves more evenly with the stagger angle, which is more appropriate for the VANT. The efficiency characteristic maps of the new turbine with different stagger angles reveal different variation law of the efficiency with expansion ratios and speeds. Along with the massflow and power characteristic maps, the results verify that the new turbine has satisfied the aerodynamic demands under two objective conditions, and performs well in a wide operating range. The fluctuation of efficiency and mass flow is great in the new turbine with low bypass ratio mode which should be paid more attention.

The original turbine has high and stable efficiency in the low bypass ratio mode which is the design condition and has low efficiency in the high bypass ratio mode. And the new turbine's performance is just like a compromise of the original one. From the loss distribution at the outlet of the stator, the new turbine has more obvious loss at the shroud while the main loss of the old turbine is at the hub. The different attack angle of the rotor after the rotated stator especially in the high bypass ratio is the main reason to cause the performance difference. Because the total pressure loss at the outlet in the high bypass ratio mode is larger for the new turbine while the stage performance is better, the flows in the rotor influenced by the stagger angle needs to be paid more attention.

NOMENCLATURE

Cp	pressure coefficient
$G, \bar{G}$	massflow and reduced massflow
$L, \bar{L}$	power and reduced power
$n, \bar{n}$	wheel speed and reduced wheel speed
P_{in}^{*}	stagnant pressure at the inlet
T_{in}^{*}	stagnant temperature at the inlet
w	weighted factor
η	stagnant or overall efficiency
π	expansion ratio
π_d	design expansion ratio
P	local static pressure
ρ_{in}	density at the inlet
u_{in}	axial velocity at the inlet
λ	stagger angle
ξ	total pressure loss coefficient
μ	viscosity coefficient

REFERENCES

[1] Westmoreland, J. S., Howlett, R. A., Lohmann, R. P..

"Progress on Variable Cycle Engines". AIAA/SAE/ASME 15th joint propulsion conference. June 18-20, 1979
[2] Thomas P.Moffitt etc. "Performance of a Single-Stage Turbine as Affected by Variable Stator Area". AIAAPPNO, 69-525, 1969.
[3] French, M. W., Allen, G. L.. "NASA VCE test bed engine aerodynamic performance characteristics and results". AIAA-81-1594.
[4] Fang Changde. "Variable Cycle Engines". Gas Turbine Experiment and Research. 2008, 17 (3):1-6
[5] Liu Zhigang etc. "Design and analysis of hp-turbine for variable cycle engine". ASME GT 2010-22449,2010.
[6] Fang Xiangjun and Liu Siyong etc. "Application of a 3D Blade Design Method for Supersonic Vaneless Contra-rotating Turbine". ASME GT 2008-50510, 2008